Journal of the Ceramic Society of Japan 133 [11] 657-662 2025
DOI https://doi.org/10.2109/jcersj2.25106

JCS-Japan

FULL PAPER

Enhancement of lanthanum ion conductivity by $(40\bar{2})$ plane orientation of polycrystalline $La_4Ga_2O_9$

Kakeru Shimotsukasa[1], Daisuke Urushihara[1], Toru Asaka[1], Tohru S. Suzuki[2] and Koichiro Fukuda[1,†]

[1] Division of Advanced Ceramics, Nagoya Institute of Technology, Nagoya 466–8555, Japan
[2] Optical Ceramics Group, Research Center for Electronic and Optical Materials, National Institute for Materials Science, Tsukuba 305–0047, Japan

To enhance the conductivity of La^{3+}, the $(40\bar{2})$ plane aligned polycrystalline $La_4Ga_2O_9$ (space group $P2_1/c$) was prepared by sintering at 1673 K for 2 h after colloidal processing under a high magnetic field of 12 T. The textured polycrystal was characterized by X-ray diffraction and impedance spectroscopy with respect to the grain alignment direction. The $(40\bar{2})$ plane normal of each constituent crystal grain of the polycrystal was found to be almost parallel to the applied magnetic field. The texture fraction of $(40\bar{2})$, expressed as the Lotgering factor $f_{40\bar{2}}$, was 0.235. A comparison was made of the conductivities parallel ($\sigma_{\parallel}$) and perpendicular ($\sigma_{\perp}$) to the aligned plane normal at temperatures ranging from 673 to 1073 K. These were also compared with the conductivity (σ_r) of randomly grain-oriented $La_4Ga_2O_9$ polycrystal. The $\sigma_{\parallel}$, ranging from 1.63×10^{-7} S cm^{-1} at 623 K to 8.52×10^{-4} S cm^{-1} at 1073 K, demonstrated the highest value at each temperature, followed by σ_r and $\sigma_{\perp}$ in that order. The $\sigma_{\parallel}/\sigma_{\perp}$ ratios ranged from 10.0 at 673 K to 15.2 at 1073 K, and the $\sigma_{\parallel}/\sigma_r$ ratios ranged from 6.7 at 873 K to 8.3 at 1073 K. Since the *a*-axis is almost parallel to the $(40\bar{2})$ plane normal, the enhanced La^{3+} conductivity of the $La_4Ga_2O_9$ polycrystal has confirmed, for the first time, the prediction by the bond valence energy landscape method in the literature that La^{3+} conduction is preferential along the *a*-axis.

Key-words : Lanthanum ion conductor, Grain alignment, Anisotropy, Impedance spectroscopy

[Received August 4, 2025; Accepted August 29, 2025]

1. Introduction

Solid electrolytes, in which multivalent cations conduct at relatively high rates, are capable of high-density charge transfer and are expected to be used in high-performance electrochemical devices such as high-capacity rechargeable batteries.[1–5] One of the factors that restricts the practical application of ceramics electrolytes is the comparatively elevated operating temperatures when compared with polymer electrolytes. It may therefore be employed as a more advanced energy storage battery to supersede sodium-sulphur batteries, which presently function at 573 K.[6] In sodium-sulphur batteries, the monovalent Na^+ conducts through the β-alumina solid electrolyte. In ceramics electrolytes that conduct trivalent cations, such as La^{3+} for example, a single cation possesses the capacity to carry three times the amount of charge as Na^+.

The bond valence (BV) energy landscape method[7,8] has revealed the potential for one-dimensional conduction of trivalent rare earth ions (RE^{3+}) along the *a*-axis in the cuspidine-type compounds $RE^{3+}{}_4Ga_2O_9$ (RE = La, Pr, Nd, Sm) and $RE^{3+}{}_4Al_2O_9$ (RE = Y, Nd, Eu, Tb, Lu).[9] Indeed, La^{3+} conduction has been experimentally confirmed in the randomly grain-oriented polycrystalline $La_4Ga_2O_9$ with a relatively high transference number of 0.992. The crystal structure of $La_4Ga_2O_9$ (space group $P2_1/c$) was first determined by Kasunič et al. in 2009,[10] who elucidated the presence of four La sites, two Ga sites, and nine O sites, with all identical site symmetry of Wyckoff position 4*e*. The fractional coordinates of these fifteen independent crystallographic sites were standardized according to the rules developed by Parthé and Gelato[11] and the results are presented in Table S1.[9] The crystal structure drawn using the standardized fractional coordinates consists of the 6- to 8-coordinated La polyhedra [La1O_7], [La2O_6], [La3O_8] and [La4O_7], and the 4-coordinated Ga tetrahedra [Ga1O_4] and [Ga2O_4] (Fig. S1). The BV energy isosurface for La^{3+} has demonstrated that only La^{3+} at the La1 and La2 sites contributes to the conduction along the *a*-axis, while that at La3 and La4 does not.[9] When the polycrystalline $La_4Ga_2O_9$ was electrolyzed at 10 V and 1073 K, the reaction $La_4Ga_2O_9 \rightarrow 2LaGaO_3 + La_2O_3$ occurred, producing the crystalline $LaGaO_3$ on the anode side and the La_2O_3-rich deposit on the cathode side. The formation of these two compounds has indicated that precisely half of the La ions that constitute $La_4Ga_2O_9$ contribute to conduction, which is in complete accordance with the conduction mechanism predicted by the BV energy landscape method. In addition to $La_4Ga_2O_9$, the only other compound reported

† Corresponding author: K. Fukuda; E-mail: fukuda.koichiro@nitech.ac.jp

as a La^{3+} conductor is $La_{1/3}Zr_2(PO_4)_3$.[12] In this particular NASICON-type compound, La^{3+} conducts in three dimensions, indicating that the orientation of this polycrystalline material does not enhance conductivity. However, it has been anticipated that there will be a further improvement in the conductivity of La^{3+} in the oriented polycrystalline $La_4Ga_2O_9$, in which each crystal grain comprising the polycrystal is almost oriented in the *a*-axis direction.

In ceramics, the orientation of constituent crystal grains has been demonstrated to exert a substantial influence on the material properties. The anisotropy of the physical properties of individual grains can be significantly enhanced by uniaxial alignment, which can improve the overall performance of the ceramics. A variety of methodologies have therefore been employed to orientate the crystal grains that comprise ceramics, including templated grain growth,[13,14] hot forging,[15] reactive diffusion,[16] and sintering after colloidal processing under a strong magnetic field.[17,18] The latter method exploits the phenomenon whereby single crystal particles of weakly magnetic materials with very low magnetic susceptibility, such as diamagnetic and paramagnetic crystals, rotate in a strong magnetic field generated by a superconducting magnet.[19] The $CaAl_4O_7$ crystal (space group $C2/c$) has been demonstrated to conduct Ca^{2+}.[20] Furthermore, the magnetic torque generated in a strong magnetic field has been found to align the *b*-axis in the direction of the applied magnetic field.[21] This property has been successfully employed to prepare the *b*-axis aligned $CaAl_4O_7$ polycrystal by means of sintering following colloidal processing under a strong magnetic field.[21] The anisotropy of the Ca^{2+} conductivity of the fabricated textured polycrystal has been consistent with the conduction pathways being parallel to the ⟨101⟩ direction, as indicated by the BV energy isosurface of Ca^{2+}.

In the present study, the La^{3+} conduction anisotropy of $La_4Ga_2O_9$ has been demonstrated for the first time in the (40$\bar{2}$) plane aligned polycrystal fabricated by sintering after the application of a strong magnetic field. As the (40$\bar{2}$) plane normal is almost parallel to the *a*-axis, which is the conduction direction depicted by the BV energy isosurface for La^{3+}, the conductivity along this direction of the textured polycrystal has been enhanced in comparison to the conductivity of the randomly grain-oriented $La_4Ga_2O_9$ polycrystal.

2. Experimental

2.1 Materials

The reagent-grade chemicals of La_2O_3 (99.99 %, Kishida Chemical Co. Ltd., Osaka, Japan) and Ga_2O_3 (99.99 %, Kojundo Chemical Laboratory Co. Ltd., Saitama, Japan) were utilized as starting materials and weighed in the molar ratio [La_2O_3:Ga_2O_3] = [2:1]. The starting powders were well mixed using a planetary ball mill (P-7, Fritsch, Idar-Oberstein, Germany), heated at 1573 K for 20 h, followed by quenching in air. The slightly sintered polycrystalline material thus obtained was subjected to pulverization using the ball mill in order to produce the fine powder consisting exclusively of $La_4Ga_2O_9$. The powder specimen (designated S-A) was sieved using a sieve with a 20 μm mesh opening and then further ground using the ball mill to prepare the fine powder, a part of which was observed by a scanning electron microscope (SEM: model JSM-6500F, JEOL Ltd., Tokyo, Japan). The outer shape of the 1264 crystal grains in the SEM image was analyzed using the AI Particle Analyzing Software (AIPAS, BLUE TAG Co., Ltd. Tokyo, Japan) to obtain the particle size distribution (Fig. S2). The particle size corresponding to a cumulative frequency of 50 % (D50) was found to be 0.85 μm, with a maximum particle size of approximately 5 μm or less. A part of the powder sample S-A was dispersed through the process of mutual electrostatic repulsion in distilled water, with the addition of an appropriate amount of polymeric dispersant. A static magnetic field of 12 T was applied in a parallel manner to the casting direction of the well-dispersed suspension during the slip-casting process. Previous literature provides comprehensive details regarding the high magnetic field apparatus and the preparation procedure for the suspension.[17] The crystal particles of $La_4Ga_2O_9$ in the suspension were oriented in the strong magnetic field, suggesting that $La_4Ga_2O_9$ is diamagnetic like Al_2O_3.[18] The resulting green body was then heated at 1673 K for 2 h in the absence of the magnetic field to prepare the disc-shaped sintered polycrystal (termed S-B) with a diameter of 10.6 mm and a thickness of 2.0 mm. The table plane was perpendicular to the direction of the applied magnetic field [Fig. S3(a)].

The residual part of sample S-A was compressed into a pellet, heated at 1673 K for 20 h, followed by quenching in air to obtain the disc-shaped sintered $La_4Ga_2O_9$ polycrystal (termed S-C) with random grain orientation (φ5.5 mm and 2.0 mm thick).

2.2 Characterization

The resulting sintered polycrystal of S-B was cut into two pieces using a diamond saw perpendicular to the table plane [Fig. S3(b)]. X-ray diffraction (XRD) patterns were collected separately from the table plane and the cross-sectional surface using a diffractometer with Bragg-Brentano geometry (model X'Pert PRO Alpha-1, PANalytical B.V., Almelo, The Netherlands). The incident Cu Kα_1 beam was maintained at a constant irradiation length of 5 mm on the sample surface by an automatic diverging slit. Since the X-ray beam width was 5 mm, the area analyzed was approximately 25 mm^2. Continuous scanning was used with an experimental 2θ range from 10.0 to 88.0°. The integrated reflection intensities were extracted by the Le Bail method[22] using the computer program RIETAN-FP.[23] The XRD pattern with $10.0° \leq 2\theta \leq 80.8°$ was obtained from the table plane of the disc-shaped sintered polycrystal of S-C. The integrated intensities of individual reflections were derived by the Le Bail method.

The X-ray powder diffraction (XRPD) pattern of S-A was collected in the 2θ range of 10.0–88.0°, and the unit cell dimensions were refined by the Le Bail method using the computer program RIETAN-FP. The RIETAN-FP

program was also utilized for the simulation of the XRD intensities of polycrystalline models with random and aligned crystal orientation, based on the standardized structural parameters of $La_4Ga_2O_9$ (Table S1). We have developed two polycrystalline models. The first model, designated model **1**, consists of the aligned platelet crystals with a well-developed $(40\bar{2})$ cleavage plane, and the second model, designated model **2**, consists of the aligned needle-like crystals elongated along the $(40\bar{2})$ plane normal. Following the requirement of the March-Dollase function[24,25] built into RIETAN-FP, the preferred orientation vector was set to be a reciprocal lattice vector, $4a^* + 0b^* - 2c^*$, perpendicular to the $(40\bar{2})$ plane for both polycrystalline models. The parameter r, representing the effective sample compression in model **1** ($r \leq 1$), was set to 0.1, 0.5, and 1 with decreasing degree of orientation. In the crystalline model exhibiting no preferred orientation, r is equal to one. In model **2** ($r \geq 1$) the parameter r, which is representative of the extension due to preferred orientation, was set to 5 and 1.8, with the orientation degree higher for the former than for the latter.

The texture fraction in the $(40\bar{2})$ plane was determined by the Lotgering method.[26] This process involved the collection of *hkl* reflection intensities from the table plane of the textured specimen and the simulation of *hkl* reflection intensities of the polycrystalline model with random grain orientation. The Lotgering factor $f_{40\bar{2}}$ is defined by the following equation:

$$f_{40\bar{2}} = (P_{40\bar{2}} - P_0)/(1 - P_0) \quad (1)$$

where

$$P_{40\bar{2}} = (\Sigma\, I_{40\bar{2}})/(\Sigma\, I_{hkl}),$$

and

$$P_0 = (\Sigma\, I^0{}_{40\bar{2}})/(\Sigma\, I^0{}_{hkl}).$$

The I_{hkl} and $I^0{}_{hkl}$ represent the observed and the simulated intensities of *hkl* peaks, respectively. The $f_{40\bar{2}}$-values were also derived using Eq. (1) for the simulated XRD patterns of the polycrystalline model **1** with different degrees of orientation.

One of the cut specimens of S-B was subjected to further division into two pieces using a diamond saw. One piece was then mechanically polished parallel to the original table plane using SiC abrasive paper, followed by a mirror-polished finish with diamond paste, to prepare the thin plate electrolyte with a thickness (L) of 0.202 cm, surface area (S) of 9.31×10^{-2} cm^2, and shape factor (L/S) of 2.17 cm^{-1}. This specimen was designated electrolyte **1**. The other piece was polished parallel to the original cross-sectional surface to make the thin plate electrolyte (designated electrolyte **2**) with $L/S = 2.81$ cm^{-1} ($L = 19.60 \times 10^{-2}$ cm and $S = 6.98 \times 10^{-2}$ cm^2). The preparation of the plate electrodes involved the application of platinum paste to both sides of electrolyte **1** and electrolyte **2**, followed by heating at 1273 K. During this process, the paste decomposed and the platinum residue hardened to form the platinum electrode. Complex impedance data were collected using an impedance analyzer (IM3570, HIOKI E. E. Co., Nagano, Japan) at temperatures ranging from 623 to 1073 K over the frequency range of 4 to 5 M Hz in air. A calibrated type K thermocouple was positioned in close proximity to the sample to ensure precise temperature measurements. The impedance spectra were subjected to a non-linear least squares fitting process utilizing ZView software.[27] In the adopted equivalent circuit, the elements corresponding to conductor-derived equipment (eq), bulk, and grain boundary (gb) are connected in series as $R_{eq}(R_{bulk}Q_{bulk})(R_{gb}Q_{gb})$, where R is the resistance in parallel with the constant phase element Q.

The table planes of sample S-C were mirror-polished with diamond paste, thus producing a disc-shaped electrolyte for the collection of complex impedance data. Since the distance between electrodes L was 19.60×10^{-2} cm and the electrode area S was 8.49×10^{-1} cm^2, the shape factor L/S was determined to be 2.31×10^{-1} cm^{-1}. The platinum electrodes were prepared on the polished table planes according to the previously outlined method.

The calculation of the spatial distribution of the BV energy for La^{3+} in the crystal structure of $La_4Ga_2O_9$ was performed using a computer program PyAbstantia.[28] The BV energy isosurface and the ball-and-stick structural model, as well as the arrangement of the $(40\bar{2})$ plane relative to the BV energy isosurface for La^{3+}, were visualized using a software VESTA.[29]

3. Results and discussion

3.1 $(40\bar{2})$ plane aligned polycrystal and orientation degree

The refined unit-cell dimensions of the $La_4Ga_2O_9$ sample S-A were in fair agreement with the reported values in the literature (Table S2).[9,10] The refinement result was satisfactory, as evidenced by the relatively low R and S values of $R_{wp} = 6.833$ %, $R_p = 5.1240$ %, and $S = 1.1545$, with no reflections from any impurities (Fig. S4). As illustrated in **Fig. 1**, the interior of the BV energy isosurface corresponds to the conduction path of La^{3+}. This figure clearly demonstrates that La^{3+} in only the La1 and La2 sites conducts in the a-axis direction, while La^{3+} in the La3 and La4 sites does not contribute to conduction. This is in full agreement with the conclusion of the preceding study.[9] The angle at which the a-axis intersects the $(40\bar{2})$ plane was determined using the refined lattice constants and found to be nearly perpendicular to the $(40\bar{2})$ plane at 89.406(3)°. It should be noted here that if La^{3+} conducts along the a-axis almost perpendicularly to the $(40\bar{2})$ plane, then the closer the $f_{40\bar{2}}$-value is to 1, the higher the ionic conductivity is expected to be.

The XRD pattern taken from the table plane of the textured sample actually demonstrated the reflections $22\bar{1}$ and $62\bar{3}$ in addition to the most intense $40\bar{2}$ reflection, and the $f_{40\bar{2}}$-value was determined to be 0.235 [**Fig. 2**(a)]. When the $(40\bar{2})$ planes of the crystal grains comprising the polycrystal are fully oriented, the $f_{40\bar{2}}$-value becomes 1, and only the $40\bar{2}$ reflection will be observed, as demonstrated by the simulated XRD pattern of the polycrystal-

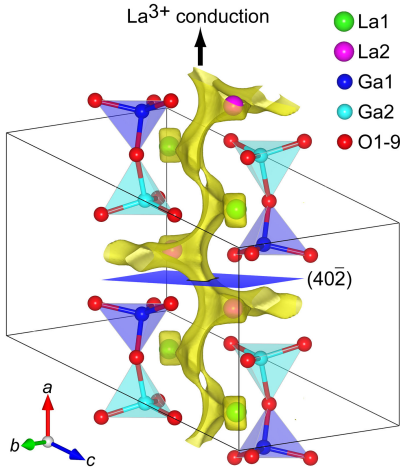

Fig. 1. Isosurface of BV energy for La^{3+} (Isovalue −1.60 eV, E_{min} −8.53 eV) showing the infinite connectivity of the La^{3+} conduction pathway along the *a*-axis in $La_4Ga_2O_9$. The angle between the *a*-axis and the (40$\bar{2}$) plane is 89.406(3)°, indicating that the conduction pathway and the (40$\bar{2}$) plane are nearly orthogonal. The parallelepiped drawn with solid lines represents the unit cell [$a = 0.79778(3)$ nm, $b = 1.12049(4)$ nm, $c = 1.16198(4)$ nm, and $\beta = 109.482(2)°$]. The structural model and isosurface visualized using a computer program VESTA.[28)]

line model **1** with $f_{40\bar{2}} = 1.00$ ($r = 0.1$) [Fig. S5(a)]. The simulations also show that, as the degree of (40$\bar{2}$) plane orientation decreased with $f_{40\bar{2}} = 0.20$ ($r = 0.5$), the reflections other than 40$\bar{2}$, such as 22$\bar{1}$ and 62$\bar{3}$, become more prominent [Fig. S5(b)]. This simulated XRD pattern was similar in profile shape to the XRD pattern of the textured sample, so they showed the comparable $f_{40\bar{2}}$-values. As demonstrated in Fig. 2(a) inset and Fig. S5(c), the simulated XRD patterns for $f_{40\bar{2}} = 0$ ($r = 1$), corresponding to the XRD pattern of randomly grain-orientated $La_4Ga_2O_9$ polycrystal, show that the reflection indices of the strongest peak are 22$\bar{1}$ with the 40$\bar{2}$ reflection still clearly recognized. Therefore, the texture fraction of the (40$\bar{2}$) plane is also quantified by the integrated intensity ratio of $I_{40\bar{2}}/I_{22\bar{1}}$. The $I_{40\bar{2}}/I_{22\bar{1}}$ ratio for the randomly grain-oriented polycrystalline model **1** ($f_{40\bar{2}} = 0$ and $r = 1$) is 0.184 [Fig. S5(c)]. For the current textured specimen, the integrated intensity of the 40$\bar{2}$ reflection exhibited a significant increase relative to that of the 22$\bar{1}$ reflection, resulting in a substantially higher $I_{40\bar{2}}/I_{22\bar{1}}$ ratio of 5.34 [Fig. 2(a)].

In the event of the (40$\bar{2}$) plane normal of each crystal grain comprising the polycrystal being perfectly oriented, the XRD pattern should exhibit an absence of 40$\bar{2}$ reflection, with only the 0*kl* reflections being observed. This is

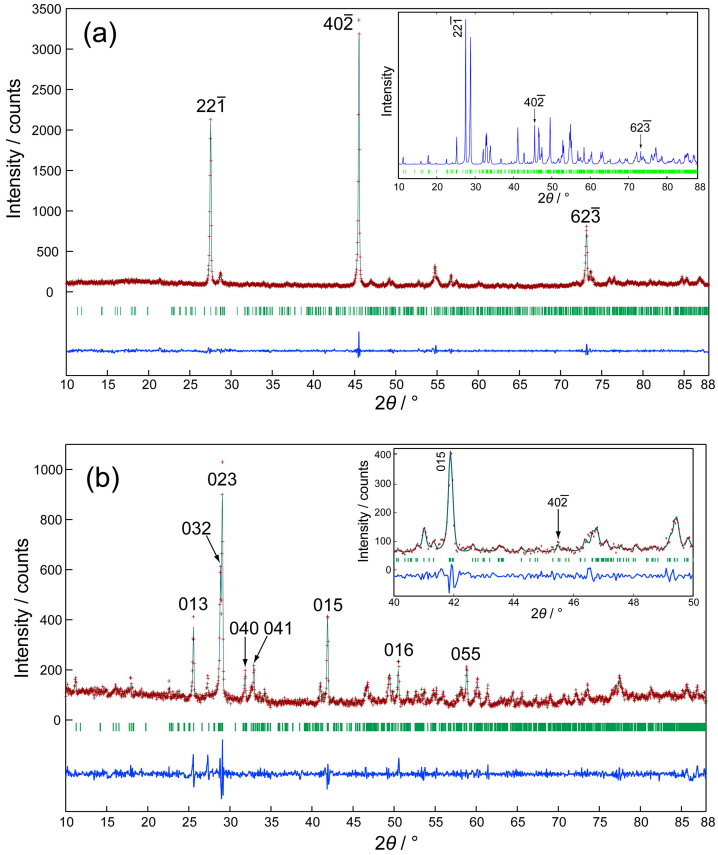

Fig. 2. The fitting results of the X-ray diffraction patterns (red symbols: +) of the disc-shaped sintered polycrystal. The irradiated surface areas correspond to the table plane in (a) and the cross section in (b). In each figure, the calculated pattern and the possible locations of the Bragg reflections are indicated by solid lines at the top and vertical bars at the bottom, respectively, while the difference curve is shown at the bottom of the figure. Inset in (a): The simulated X-ray diffraction pattern of the randomly grain-oriented $La_4Ga_2O_9$ polycrystal. Inset in (b): Magnified view for $40° \leq 2\theta \leq 50°$.

demonstrated by the simulated XRD pattern of the polycrystalline model **2** with $r = 5$ [Fig. S6(a)]. Conversely, in model **2** with the lower orientation degree of $r = 1.8$, the $40\bar{2}$ reflection is clearly observed [Fig. S6(b)], although its diffraction intensity is extremely low. The XRD pattern obtained from the cross-sectional surface of the cut sample exhibited a very weak $40\bar{2}$ reflection, with the $0kl$ reflections being predominantly observed [Fig. 2(b)]. This finding is consistent with the simulated XRD pattern of the polycrystalline model **2** with $r = 1.8$. It is noteworthy that the crystal grains comprising the polycrystalline model **2** have an overall random orientation of their *b*-axis direction around the $(40\bar{2})$ plane normal. Therefore, the close similarity between the observed XRD pattern [Fig. 2(b)] and the simulated XRD pattern [Fig. S6(b)] suggests that the textured sample is composed of the crystal grains with randomly oriented *b*-axis directions around the common $(40\bar{2})$ plane normal.

The $f_{40\bar{2}}$-value obtained from the XRD intensities of the S-C polycrystal (Fig. S7) according to Eq. (1) was 0.01. This confirms that the S-C is composed of the $La_4Ga_2O_9$ crystals with random grain orientation.

3.2 Anisotropy of La^{3+} conduction

The bulk conductivity of electrolyte **1** ($\sigma_{\parallel}$) corresponds to the La^{3+} conductivity parallel to the direction in which the $(40\bar{2})$ plane normal of the constituent crystal grains are moderately oriented at $f_{40\bar{2}} = 0.235$, while the bulk conductivity of electrolyte **2** ($\sigma_{\perp}$) corresponds to the La^{3+} conductivity perpendicular to this direction (**Fig. 3**). The $\sigma_{\parallel}$ and $\sigma_{\perp}$ values at 623–1073 K were derived from the corresponding R_{bulk} values at each temperature of electrolyte **1** and electrolyte **2**, respectively (Figs. S8 and S9). The $\sigma_{\parallel}$-value exhibited a steady increase from 1.63×10^{-7} S cm^{-1} at 623 K to 8.52×10^{-4} S cm^{-1} at 1073 K with increasing temperature. The activation energy of conduction

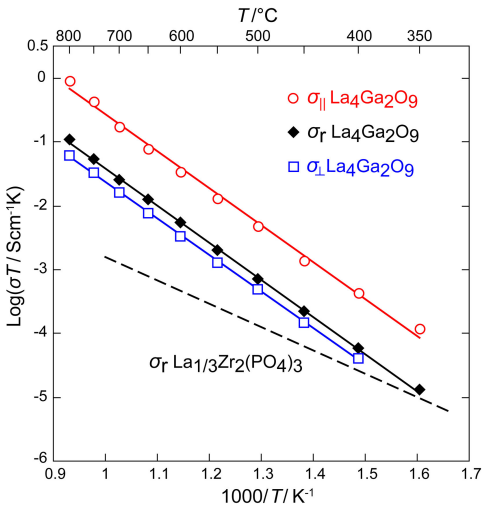

Fig. 3. Anisotropy of La^{3+} conduction in the $(40\bar{2})$ plane aligned $La_4Ga_2O_9$ polycrystal. The bulk conductivity $\sigma_{\parallel}$ (electrolyte **1**) is parallel to the aligned plane normal, and that of $\sigma_{\perp}$ (electrolyte **2**) is perpendicular to it. The bulk conductivities for randomly grain-oriented polycrystals (σ_r) are shown for $La_4Ga_2O_9$ and $La_{1/3}Zr_2(PO_4)_3$.

(E_1) was determined to be 1.16(2) eV from the Arrhenius plot. The $\sigma_{\perp}$-value also increased steadily from 5.92×10^{-8} to 5.62×10^{-5} S cm^{-1} with increasing temperature from 673 to 1073 K, with the E_2-value of 1.14(1) eV. The bulk conductivity of S-C (σ_r) was determined from the corresponding R_{bulk} values at each temperature (Fig. S10). It increased steadily from 2.08×10^{-8} S cm^{-1} (623 K) to 1.03×10^{-4} S cm^{-1} (1073 K) with increasing temperature, with the E_r-value of 1.15(1) eV. The activation energies, E_1, E_2, and E_r, were found to be almost identical among the three. It is hypothesized that these values correspond to the activation energy required for the conduction of La^{3+}, occupying the La1 and La2 sites, in the *a*-axis direction. On the other hand, the value of the activation energy E_{BV}, as estimated by the BV energy landscape method, has been determined to be 6.55 eV.[9] Therefore, the value of the scaling factor required to convert the E_{BV} value to the actual activation energy value is approximately 0.176 (= 1.15/6.55).

If the direction of La^{3+} conduction were restricted to the $(40\bar{2})$ normal direction, for the perfectly $(40\bar{2})$ plane aligned polycrystal with $f_{40\bar{2}} = 1$, the $\sigma_{\perp}$-value should be zero. However, the actual $f_{40\bar{2}}$-value was found to be equal to 0.235, strongly suggesting that the conduction pathways contributing to $\sigma_{\perp}$ are formed within the present textured polycrystal. When compared at the same temperatures, the $\sigma_{\parallel}$-values were about 10.0 (673 K) to 15.2 (1073 K) times higher than the $\sigma_{\perp}$-values. This provides strong evidence that the conduction of La^{3+} in the crystal structure of $La_4Ga_2O_9$ occurs predominantly along the *a*-axis. The conductivity of the randomly grain-oriented polycrystal (σ_r) of $La_4Ga_2O_9$ was intermediate between $\sigma_{\parallel}$ and $\sigma_{\perp}$, with the $\sigma_{\parallel}/\sigma_r$ ratios ranging from 6.7 (873 K) to 8.3 (1073 K). A comparison of the σ_r values of $La_{1/3}Zr_2(PO_4)_3$[12] with those of $\sigma_{\parallel}$ at each temperature from 623 to 973 K revealed that the latter were approximately 10.5 (623 K) to 132 (973 K) times higher than the former.

Observation of the crystal structure of $La_4Ga_2O_9$ from the reciprocal *c*-axis (c^*-axis) direction reveals a layered structure (layer thickness of approximately 4.0 nm) parallel to the $(40\bar{2})$ plane, which is nearly perpendicular to the *a*-axis (Fig. S11). This layer is arranged in two pieces for the unit cell period along the *a*-axis direction, forming the entire crystal structure. The observed alignment of the $(40\bar{2})$ layer with the direction of the applied magnetic field indicates that the magnetic field would generate a magnetic torque on the $(40\bar{2})$ layer, causing the normal direction of the $(40\bar{2})$ layer to align with the direction of the magnetic field. The crystalline particle size has the potential to influence the effect of torque rotation of the particles. It can be hypothesized that smaller particles are more susceptible to the effects of magnetic torque. However, further research is needed to clarify the details of the particle alignment process caused by the application of a strong magnetic field.

The BV energy landscape method was the first to demonstrate the possibility of RE^{3+} conduction along the *a*-axis in the cuspidine-type compounds $RE^{3+}{}_4Ga_2O_9$ (RE =

La, Pr, Nd, Sm) and $RE^{3+}{}_4Al_2O_9$ (RE = Y, Nd, Eu, Tb, Lu).[9] In the present study, the conduction anisotropy of La^{3+} in $La_4Ga_2O_9$ has been experimentally confirmed for the first time, providing strong support for the hypothesis that the conduction direction is primarily along the a-axis. In the sample prepared for this study, the $f_{40\bar{2}}$-value was 0.235, which is considerably less than 1. The precise cause of this remains to be elucidated; however, it is conceivable that the dispersion of the crystal particles in the suspension during the application of the magnetic field was inadequate. If a sample with the highly (40$\bar{2}$) plane orientation can be obtained in which the $f_{40\bar{2}}$-value is close to 1, then a further improvement in ionic conductivity can be expected. This objective could be realized through the improvement of the suspension dispersion process by optimizing the particle size distribution of the powder and/or the amount of polymeric dispersant added.

4. Conclusion

The (40$\bar{2}$) plane aligned polycrystalline $La_4Ga_2O_9$ (space group $P2_1/c$) was prepared by sintering at 1673 K for 2 h, following colloidal processing under the high magnetic field of 12 T. In the course of the slip-casting process, the dispersed particle suspension exhibited a tendency to align the normal direction of each grain's (40$\bar{2}$) plane with the static applied magnetic field, which was oriented parallel to the direction of particle settlement. Therefore, following sintering in the absence of a magnetic field, the resulting polycrystal exhibited a moderate (40$\bar{2}$) plane orientation, as evidenced by the Lotgering factor $f_{40\bar{2}}$ of 0.235. The conductivities parallel ($\sigma_{\parallel}$) and perpendicular ($\sigma_{\perp}$) to the aligned plane normal were compared at temperatures ranging from 673 to 1073 K, together with the conductivity (σ_r) of randomly grain-oriented polycrystal. The $\sigma_{\parallel}$-value increased steadily from 1.63×10^{-7} to 8.52×10^{-4} S cm^{-1} with increasing temperature from 623 K to 1073 K. The activation energy for conduction was determined to be 1.16(2) eV. When compared at the same temperatures, $\sigma_{\parallel}$ was the highest, followed by σ_r and then $\sigma_{\perp}$ in that order. The present study has confirmed for the first time the anisotropy of La^{3+} conduction in $La_4Ga_2O_9$, and the obtained results were consistent with the preferential a-axis conduction predicted by the BV energy landscape method. If the polycrystals with the higher degree of (40$\bar{2}$) plane orientation can be prepared by the improved colloidal processing under high magnetic field, a further enhancement of the conductivity would be expected.

Appendix A. Supporting information
Supplementary data associated with this article can be found in the on line version.

References

1) L. F. O'Donnell and S. G. Greenbaum, *Batteries* 7, 3 (2021).
2) Y. Liang, H. Dong, D. Aurbach and Y. Yao, *Nat. Energy* 5, 646 (2020).
3) A. Ponrouch, J. Bitenc, R. Dominko, N. Lindahl, P. Johansson and M. R. Palacín, *Energy Storage Mater.* 20, 253 (2019).
4) N. Imanaka and S. Tamura, *B. Chem. Soc. Jpn.* 84, 353 (2011).
5) N. Imanaka, *J. Ceram. Soc. Jpn.* 113, 387 (2005).
6) D. Kumar, S. K. Rajouria, S. B. Kuhar and D. K. Kanchan, *Solid State Ionics* 312, 8 (2017).
7) S. Adams and R. P. Rao, *Phys. Status Solidi A* 208, 1746 (2011).
8) S. Adams and R. P. Rao, Understanding Ionic Conduction and Energy Storage Materials with Bond-Valence-Based Methods, in "Bond Valences", Ed. by I. D. Brown and K. R. Poeppelmeier, Springer, Berlin Heidelberg (2014) pp. 129–159.
9) K. Shimotsukasa, D. Urushihara, T. Asaka and K. Fukuda, *Chem. Mater.* 36, 4821 (2024).
10) M. Kasunič, A. Meden, S. D. Škapin, D. Suvorov and A. Golobič, *Acta Crystallogr. B* 65, 558 (2009).
11) E. Parthé and L. M. Gelato, *Acta Crystallogr. A* 40, 169 (1984).
12) M. Barré, F. Le Berre, M. P. Crosnier-Lopez, O. Bohnke, J. Emery and J. L. Fourquet, *Chem. Mater.* 18, 5486 (2006).
13) H. Igarashi, K. Matsunaga, T. Taniai and K. Okazaki, *Am. Ceram. Soc. Bull.* 57, 815 (1978).
14) M. Holmes, R. E. Newnham and L. E. Cross, *Am. Ceram. Soc. Bull.* 58, 872 (1979).
15) T. Takenaka and K. Sakata, *Jpn. J. Appl. Phys.* 19, 31 (1980).
16) K. Fukuda, T. Asaka, R. Hamaguchi, T. Suzuki, H. Oka, A. Berghout, E. Béchade, O. Masson, I. Julien, E. Champion and P. Thomas, *Chem. Mater.* 23, 5474 (2011).
17) T. S. Suzuki, *J. Ceram. Soc. Jpn.* 128, 1005 (2020).
18) T. S. Suzuki, T. Uchikoshi and Y. Sakka, *Sci. Technol. Adv. Mat.* 7, 356 (2006).
19) T. Sugiyama, M. Tahashi, K. Sassa and S. Asai, *ISIJ Int.* 43, 855 (2003).
20) K. Fukuda, R. Harada, H. Banno, D. Urushihara and T. Asaka, *ACS Appl. Energ. Mater.* 5, 3227 (2022).
21) K. Fukuda, F. Nakajima, D. Urushihara, T. Asaka, T. S. Suzuki, A. Berghout, A. Bouzid, O. Masson and P. Thomas, *J. Ceram. Soc. Jpn.* 137, 409 (2024).
22) A. Le Bail, H. Duroy and J. L. Fourquet, *Mater. Res. Bull.* 23, 447 (1988).
23) F. Izumi and K. Momma, *Solid State Phenom.* 130, 15 (2007).
24) A. Z. March, *Z. Krist.-Cryst. Mater.* 81, 285 (1932).
25) W. A. Dollase, *J. Appl. Crystallogr.* 19, 267 (1986).
26) F. K. Lotgering, *J. Inorg. Nucl. Chem.* 9, 113 (1959).
27) D. Johnson, ZView Program (Version 2.9b), Scribner Associ-ates Inc., Southern Pines, NC (1990).
28) P. Barpanda, G. Oyama, S. Nishimura, S.-C. Chung and A. Yamada, *Nat. Commun.* 5, 4358 (2014).
29) K. Momma and F. Izumi, *J. Appl. Crystallogr.* 44, 1272 (2011).